 Q. J. R. Meteorol. Soc. 142: 1890–1903, July 2016 A DOI:10.1002/qj.2782

RMetS
Royal Meteorological Society

Eleven-year solar cycle signal in the NAO and Atlantic/European blocking

L. J. Gray,[a,b]* T. J. Woollings,[b] M. Andrews[c] and J. Knight[c]
[a]*NERC National Centre for Atmospheric Science (NCAS), UK*
[b]*Atmospheric, Oceanic and Planetary Physics, University of Oxford, UK*
[c]*Hadley Centre, Met Office, Exeter, UK*

*Correspondence to: L. J. Gray, Physics Department, Clarendon Laboratory, Oxford University, Parks Road, Oxford OX1 3PU.
E-mail: gray@atm.ox.ac.uk

The 11-year solar cycle signal in December–January–February (DJF) averaged mean-sea-level pressure (SLP) and Atlantic/European blocking frequency is examined using multilinear regression with indices to represent variability associated with the solar cycle, volcanic eruptions, the El Niño–Southern Oscillation (ENSO) and the Atlantic Multidecadal Oscillation (AMO). Results from a previous 11-year solar cycle signal study of the period 1870–2010 (140 years; ∼13 solar cycles) that suggested a 3–4 year lagged signal in SLP over the Atlantic are confirmed by analysis of a much longer reconstructed dataset for the period 1660–2010 (350 years; ∼32 solar cycles). Apparent discrepancies between earlier studies are resolved and stem primarily from the lagged nature of the response and differences between early- and late-winter responses. Analysis of the separate winter months provide supporting evidence for two mechanisms of influence, one operating via the atmosphere that maximises in late winter at 0–2 year lags and one via the mixed-layer ocean that maximises in early winter at 3–4 year lags. Corresponding analysis of DJF-averaged Atlantic/European blocking frequency shows a highly statistically significant signal at ∼1-year lag that originates primarily from the late winter response. The 11-year solar signal in DJF blocking frequency is compared with other known influences from ENSO and the AMO and found to be as large in amplitude and have a larger region of statistical significance.

Key Words: 11-year solar cycle; atmospheric variability; NAO; atmospheric blocking; solar variability; North Atlantic variability

Received 27 October 2015; Revised 16 February 2016; Accepted 29 February 2016; Published online in Wiley Online Library 13 May 2016

1. Introduction

An influence of the 11-year solar cycle on surface weather patterns over Europe has been proposed for many years, as summarised in the review by Gray *et al.* (2010). However, taking into account the Sun's variability has not become an accepted mainstream component of seasonal weather forecast models. This is partly because the globally averaged variability in incoming solar irradiance at the Earth's surface is an extremely small fraction of the total, and mechanisms for transferring the signal from the upper atmosphere and amplifying its impact at the surface are not fully understood. It is also partly because the response signature seen in observations is present in some regions but not others, and is evident during some time periods but found to be absent, or even reversed, during other time periods. Not surprisingly this has given rise to suggestions that the apparent response may be an artefact of the analysis. Nevertheless, over recent years there have been a growing number of observational studies pointing to a real influence of solar variability in certain regions including the Atlantic/European sector and further development of proposed mechanisms through which the surface signal can be amplified in certain regions.

Observational and modelling studies of Europe and the North Atlantic have suggested the presence of a positive North Atlantic Oscillation (NAO) anomaly at times of maximum solar irradiance (Smax) and a negative NAO at times of solar minimum (Smin). For example Woollings *et al.* (2010; hereafter referred to as W2010) examined the solar variability signal in December–January–February (DJF) mean-sea-level pressure (SLP) in the ERA-40 reanalysis dataset for the period 1958–2001 and found an SLP response resembling a negative NAO response following Smin. The statistically significant response was primarily centred over the Icelandic region with stronger than usual low pressure being the prime contributor to the NAO-like pattern. W2010 also examined estimates of blocking frequency and found significantly increased frequencies of blocking during Smin (see also Barriopedro *et al.*, 2008).

On the other hand, when Roy and Haigh (2010) and Gray *et al.* (2013; hereafter referred to as G2013) examined the DJF response in the much longer Hadley Centre HadSLP

dataset (1870–2010) the (zero-lag) signal over the Atlantic showed no statistical significance either at polar or subtropical latitudes. A third relevant study is that of Brugnara *et al.* (2013) who analysed an even longer time period (1749–2002) using the SLP reconstruction of Luterbacher *et al.* (2002) for January–February–March (JFM) averages. They found a statistically significant positive NAO-like anomaly coinciding with Smax periods similar to the Woollings signal, in which the response was also dominated by the Icelandic negative anomaly.

These various studies thus suggest that the solar cycle response signal may be dependent on the time period and/or the months selected for analysis. However, while the majority of observational and modelling studies have examined only the immediate (zero-lag) surface response, G2013 also examined the SLP response at different lags from 0 to 11 years, i.e. the longer-term response in the years following a peak (or trough) in solar activity. While their response at lag-zero was not significant (unlike the W2010 and Brugnara *et al*. results), they found a statistically significant positive DJF signal emerging over the Azores 2–4 years following Smax, peaking at over 3 hPa with 99% statistical significance. This response also projects onto the NAO pattern, giving a positive NAO following Smax similar to the results of W2010 and Brugnara *et al*., but the signal was delayed by 2–4 years and emanated primarily from the southern part of the NAO pattern over the Azores.

The primary purpose of this article is to resolve and understand the similarities and differences between these various studies by re-examining all of the selected time periods using the extended lagged-response analysis employed by G2013. In doing so we find that the results are no longer contradictory and confirm the presence of a 3–4 year lagged DJF surface response to the 11-year solar cycle over the European/North Atlantic sector (section 3.1). We additionally examine the contribution to the signal from individual months during the winter season and find evidence for two different influence mechanisms, one via the mixed-layer ocean (Scaife *et al.*, 2013; Andrews *et al.*, 2015) that appears to dominate in early winter and can explain the observed lagged response in DJF and a second one, possibly via the stratosphere (Kodera and Kuroda, 2002), that peaks earlier in the solar cycle at 0–2 year lags and dominates in late winter (section 3.2). The 11-year solar cycle signal in frequency of European/Atlantic blocking events is also examined to investigate whether similar influences are evident (section 3.3). Finally, the solar cycle signal in blocking frequency is compared and placed into context alongside other major factors that are known to influence blocking frequency, namely the El Niño–Southern Oscillation (ENSO) and Atlantic Multidecadal Oscillation (AMO; section 3.4). The results are summarised in section 4.

2. Datasets and methodology

Analysis of the monthly averaged gridded mean-sea-level pressure (SLP) is confined primarily to the North Atlantic–European sector (30°W–40°E; 30°N–70°N) since this is the regional extent of the reconstruction dataset of Luterbacher *et al.* (2002) which covers the extended period 1659–1999 (http://www.ncdc.noaa.gov/paleo/paleo.html; see also Kuttel *et al.*, 2010). Data for the Atlantic/European sector are also extracted from the global Hadley Centre Sea Level Pressure (HadSLP2) dataset (Allan and Ansell, 2006) for the period 1870–2004 and extended to 2010 by the HadSLP2r dataset (http://www.metoffice.gov.uk/hadobs), as in the study of Gray *et al.* (2013). Where analysis of the Luterbacher *et al*. reconstruction is shown extended to 2010 (for comparison with other datasets) the reconstruction has been extended from 1999 to 2010 using the HadSLP2r dataset. Figure 1(a) shows the climatology and standard deviation of SLP over the Atlantic/European sector for the period 1870–2010. The main features are the strong pressure gradient between the Icelandic Low and Azores High and the largest variability is found at the higher latitudes. The equivalent plots for the full period 1660–2010 show similar amplitudes and patterns.

The sea-surface temperature (SST) analyses shown in Figure 7 employed the Hadley Centre Sea Ice and Sea Surface Temperature (HadISST) dataset for 1870–2010 (Rayner *et al.*, 2003; www.metoffice.gov.uk./hadobs).

The frequency of blocking over Europe and the Atlantic over the period 1948–2010 was diagnosed using the National Centers for Environmental Prediction/National Center for Atmospheric Research (NCEP-NCAR) reanalysis (Kalnay *et al.*, 1996). The 'absolute geopotential height' method of Scherrer *et al.* (2006) was used, which identifies blocking at a point if (i) the meridional 500 hPa geopotential height gradient is reversed and (ii) the flow is westerly to the north of the point, with a height gradient stronger than 10 m per degree of latitude. A 5-day persistence criterion is then applied at each grid point. The number of blocking days in each season found by this method is then converted to a frequency by dividing by the total number of days in DJF. The climatology and standard deviation of this blocking frequency dataset is shown in Figure 1(b). Both the climatology and standard deviation feature local maxima over the North Sea and Greenland (see also figure 2(a) of Scherrer *et al.* (2006) for the ERA-40 reanalysis and figure 10 of Woollings *et al.* (2014) for the NCEP-NCAR data used here). We note that the 5-day persistence requirement is particularly stringent and identifies only the extreme events each winter. The blocking dataset contains only values of zero days or greater than 5 days. The peak climatological frequency of 5.5% suggests an average of just over one event per year but we note that this average is a combination of frequent years with no occurrences of extreme blocking events together with other years with many more days of extreme events.

The de-seasonalised SLP, SST and blocking data were analysed using the multilinear regression approach employed by Gray *et al.* (2013) (see also Crooks and Gray (2005) for a more detailed description of the methodology) in which the time series of data at each grid point are optimally fitted using a combination of indices that represent potential sources of forced variability. These indices included representation of variability associated with solar variability, volcanic eruptions, ENSO, the Quasi-Biennial Oscillation (QBO), the AMO and a long-term trend. The indices were normalised by their standard deviation prior to performing the regression analysis. Extensive sensitivity tests were performed to ensure that inclusion/exclusion of individual indices did not substantially influence the signals associated with the other indices. An autoregressive AR(1) noise model was employed. The noise coefficients were calculated simultaneously with the other components of variability and were consistent with a red noise of order one. Sensitivity tests with orders up to AR(3) did not show significant differences. A two-tailed Student's t-test was used to determine the 95% and 99% probabilities that the regression coefficients are significantly different from noise.

Figure 2 shows the 1870–2010 time series of the indices employed for the main regression analyses (volcanic, ENSO, AMO) and the 1660–2010 time series of sunspot number. The major volcanic eruptions were represented by an updated annual-averaged time series of aerosol optical depth (Sato *et al.*, 1993). ENSO variability for the period 1870–2010 was represented by monthly-averaged sea-surface temperatures from the Hadley Centre HadISST dataset (www.metoffice.gov.uk/hadobs) averaged over the Niño 3.4 region (5°S–5°N; 170–120°W). The (unsmoothed) AMO index from 1856 to the present, covering the region 0–75°N and 10°E–75°W, was acquired from NOAA (http://www.esrl.noaa.gov/psd/data/timeseries/AMO: Enfield *et al.*, 2001). The unsmoothed data were employed in all analyses but we note that sensitivity tests using the smoothed data showed that the results were unaffected by the removal of the shorter-term variations.

A linear trend was also included, to represent anthropogenic warming over the period (following both Brugnara *et al.* (2013) and Gray *et al.* (2013)). The QBO index employed in the regression analyses of the blocking frequency in section 3.4 was derived from radiosonde observations of equatorial winds, available from 1953

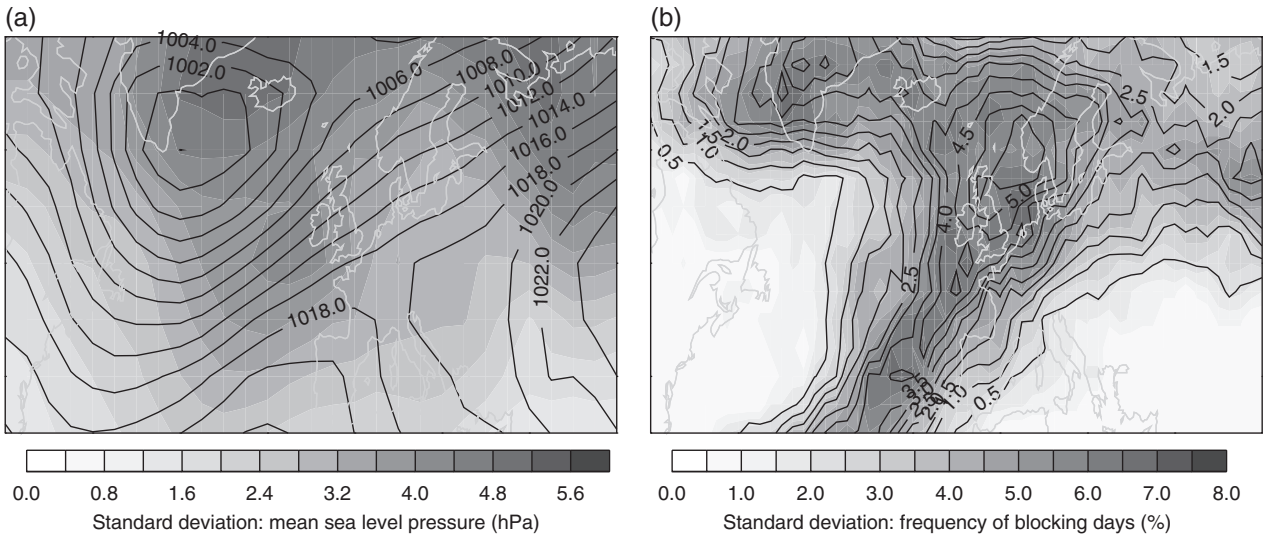

Figure 1. December–January–February averaged climatology (contours) and standard deviation (shading) for (a) mean-sea-level pressure (hPa) for the period 1870–2010, (b) blocking frequency (percentage of days) for the period 1953–2010.

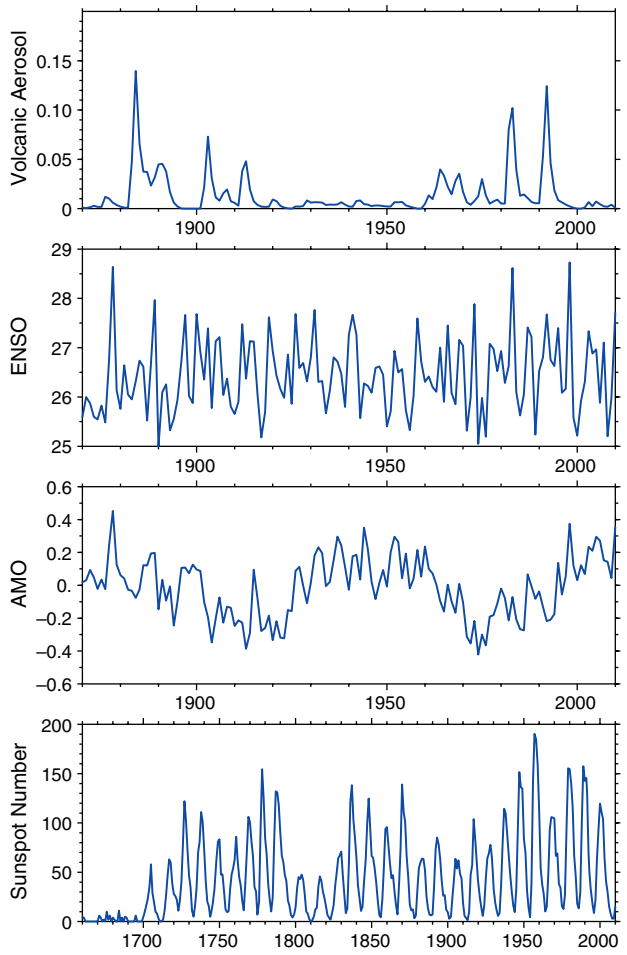

Figure 2. Time series of forcing indices employed in the regression analyses, representing variability associated with: (a) volcanic aerosol (stratospheric aerosol optical depth), (b) the El Niño–Southern Oscillation (ENSO; °C), (c) the Atlantic Multidecadal Oscillation (AMO; °C) and (d) sunspot number. Note the different time-axis for sunspot number.

to the present (http://gcmd.nasa.gov/r/d/QBO_ZONAL_WIND_INDEX.html). As described in detail in Crooks and Gray (2005) two QBO indices were employed, which were the first two Empirical Orthogonal Functions (EOFs) of the equatorial time-series. The EOFs are orthogonal (by definition), approximately one quarter of a cycle out of phase and together they provide a good representation of the evolving descent of the QBO with time.

Annual-averaged sunspot number (SSN) was employed to represent solar variability, for consistency with previous studies (including Roy and Haigh, 2010; Brugnara *et al.*, 2013; Gray *et al.*, 2013). The sunspot data were interpolated to provide seasonally averaged or monthly averaged values as required. The Wolf sunspot number available from 1700 was employed for most of the analyses (WDC-SILO, Royal Observatory of Belgium, Brussels; http://sidc.oma.be/silso/datafiles). For the analysis of data back to 1660 this was extended using the Group Sunspot Number to cover the period 1660–1700. All results have been scaled so that plots show the solar maximum (Smax) minus solar minimum (Smin) response to a solar cycle forcing with an amplitude of 180 sunspot numbers.

Since the analysis is extended back in time and covers part of the Maunder Minimum period with very few visible sunspots, we also take into account the long-term solar variability, to ensure that we only examine the 11-year solar cycle (the study of G2013 did not require this since it only extended back to 1870). The sunspot time-series was first smoothed so that only time variations greater than ∼13 years were retained. This long-term solar signal was then subtracted from the original time series to obtain a shorter-period index that we refer to as the 11-year solar signal index. Both the 11-year and long-term indices were included (as separate terms) in the regression analysis. In this article we focus only on results from the 11-year response and not the long-term solar response. Sensitivity tests showed that inclusion or exclusion of the long-term solar index in the analyses had no effect on the amplitude, pattern or statistical significance of the 11-year solar signal results; when the long-term solar index was excluded its response was simply transferred to the residual term.

In some of the analyses there was evidence of aliasing between the long-term solar signal and the AMO since these time series are similar (and indeed there have been proposals that they may be physically linked although there is still much debate on this issue; see for example discussions in Knudsen *et al.* (2014) and Menary and Scaife (2014)). There was also some evidence of aliasing between the long-term solar and linear trend terms when only the period 1955–2010 was examined (in section 3.4) since the long-term solar signal is negative and quasi-linear during this period. However, sensitivity tests showed that neither of these interactions affected the amplitude, pattern or statistical significance of the 11-year solar response.

3. Results

3.1. *DJF mean-sea-level pressure*

The DJF averaged 11-year solar cycle signal in mean-sea-level pressure (SLP) over the European/northeast Atlantic sector for

the period 1870–2010 (140 years; approximately 13 solar cycles) is shown in Figure 3. The regression analysis included the volcanic, ENSO, AMO, long-term trend and two solar indices. This is the same analysis period as examined by G2013 (see their figure 4; note also that the colour scale range is slightly different) except that only the European/Atlantic region is shown in Figure 3, to allow better comparison with results using the Luterbacher *et al.* (2002) dataset, that has a restricted latitude/longitude domain. The lag zero result shows the Smax–Smin response when the 11-year solar cycle index corresponds exactly in time with the SLP data; lags greater than zero mean that the solar index has been shifted (backwards) by the corresponding number of years to show the response in the years following an Smax. For brevity only lags up to 5 years are shown; at lags of 6–11 years the response is approximately the same as 0–5 year lags but of opposite sign, thus encompassing a complete 11-year solar cycle (see G2013 Fig. 4). Sensitivity tests (not shown) in which various of the regression indices were excluded, either singly or in combinations, confirmed that the solar cycle signal was not unduly affected, i.e. the signal(s) associated with the excluded indices were found to be assigned to the residual and did not affect the amplitude, pattern or statistical significance of the 11-year signal.

As noted earlier, the major statistically significant pattern of response in Figure 3 does not emerge until lags of 2–4 years. The dominant signal is a region of enhanced SLP centred over the Azores region and extending across into Europe. The peak response exceeds 3 hPa and is statistically significant at the 99% level at lags of 3 years. The pattern resembles a positive NAO response following Smax that maximises approximately 3–4 years after Smax. The corresponding SST patterns (not shown) are consistent with this both spatially and temporally (see G2013).

In Figure 4 we now extend the regression analysis back in time using the reconstructed Luterbacher *et al.* (2002) dataset. Since estimates of ENSO and the AMO are either unavailable or less reliable for these earlier periods we employ only the long-term trend and two solar indices in the regression analysis. The legitimacy of this was tested by repeating the 1870–2010 analysis shown in Figure 3 but with only the solar and long-term trend terms. The resulting 11-year solar cycle response was virtually identical to Figure 3, thus justifying the assumption that the ENSO, AMO and volcanic indices are not required to identify the solar response pattern.

In Figure 4(a) the DJF solar response patterns are shown for the period 1750–2010 (260 years; approx. 24 solar cycles), using the Luterbacher *et al.* (2002) reconstruction dataset. This period corresponds approximately to the period examined by Brugnara *et al.* (2013). Sensitivity tests showed that using precisely the same years as in Brugnara *et al.*, i.e. 1749–2002, made no difference. The signal pattern is similar to the 1870–2010 analysis in Figure 3 with a statistically significant positive response that emerges only at lags of 2 years and greater, maximising at a lag of 4 years with amplitude greater than 2.5 hPa and 99% statistical significance. The pattern of response is also similar to Figure 3, resembling a positive NAO response following Smax and with the high pressure anomaly extending across into Europe. Brugnara *et al.* (2013) did not examine the lagged response in their paper but have confirmed that a similar pattern emerges using their analysis technique (Brugnara, 2013). Interestingly, at lag zero Figure 4(a) shows a negative anomaly to the west of the UK but there is no statistical significance, whereas Brugnara *et al.* found a similar negative signal at lag zero but with 99% statistical significance. We note that Brugnara *et al.* analysed January–February–March (JFM) averages rather than the DJF averages shown here. This is an important difference which is discussed further in the next section.

Figure 4(b) shows the DJF solar response patterns for the period 1660–2010 (350 years; approx. 32 solar cycles). Brugnara *et al.* (2013) limited their analysis period to 1749 onwards because of the availability of monthly sunspot data from that date and also noted that this was the period when the reconstructed SLP data

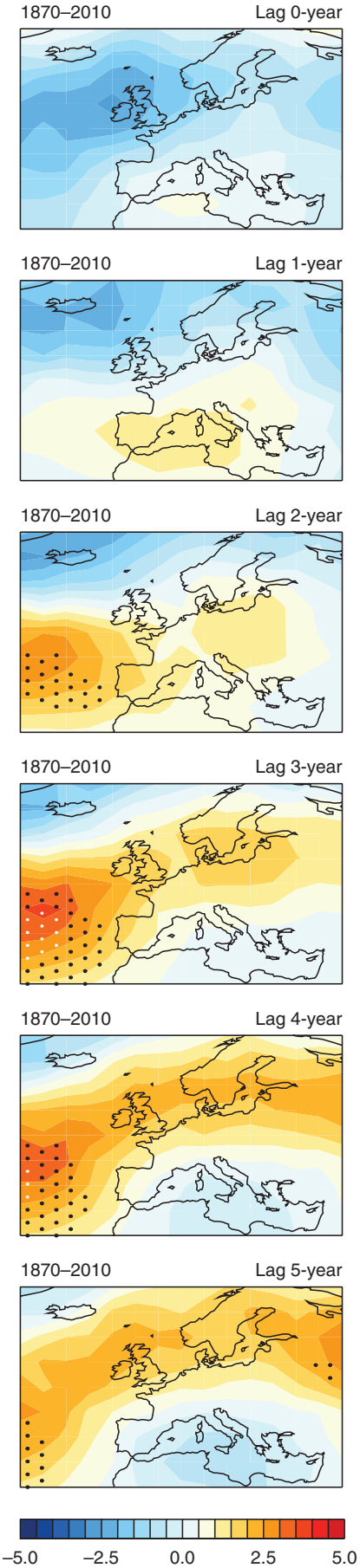

Figure 3. DJF-averaged solar cycle response (hPa) from the regression analysis of the HadSLP dataset at various lags from 0 to 5 years for the period 1870–2010. The regression coefficients have been scaled to show the response for Smax minus Smin differences of 180 sunspot numbers. Black and white stippling shows regions of 95 and 99% statistical significance, respectively. The plotted region is restricted to match that of the Luterbacher *et al.* (2002) dataset, for ease of comparison with Figure 4.

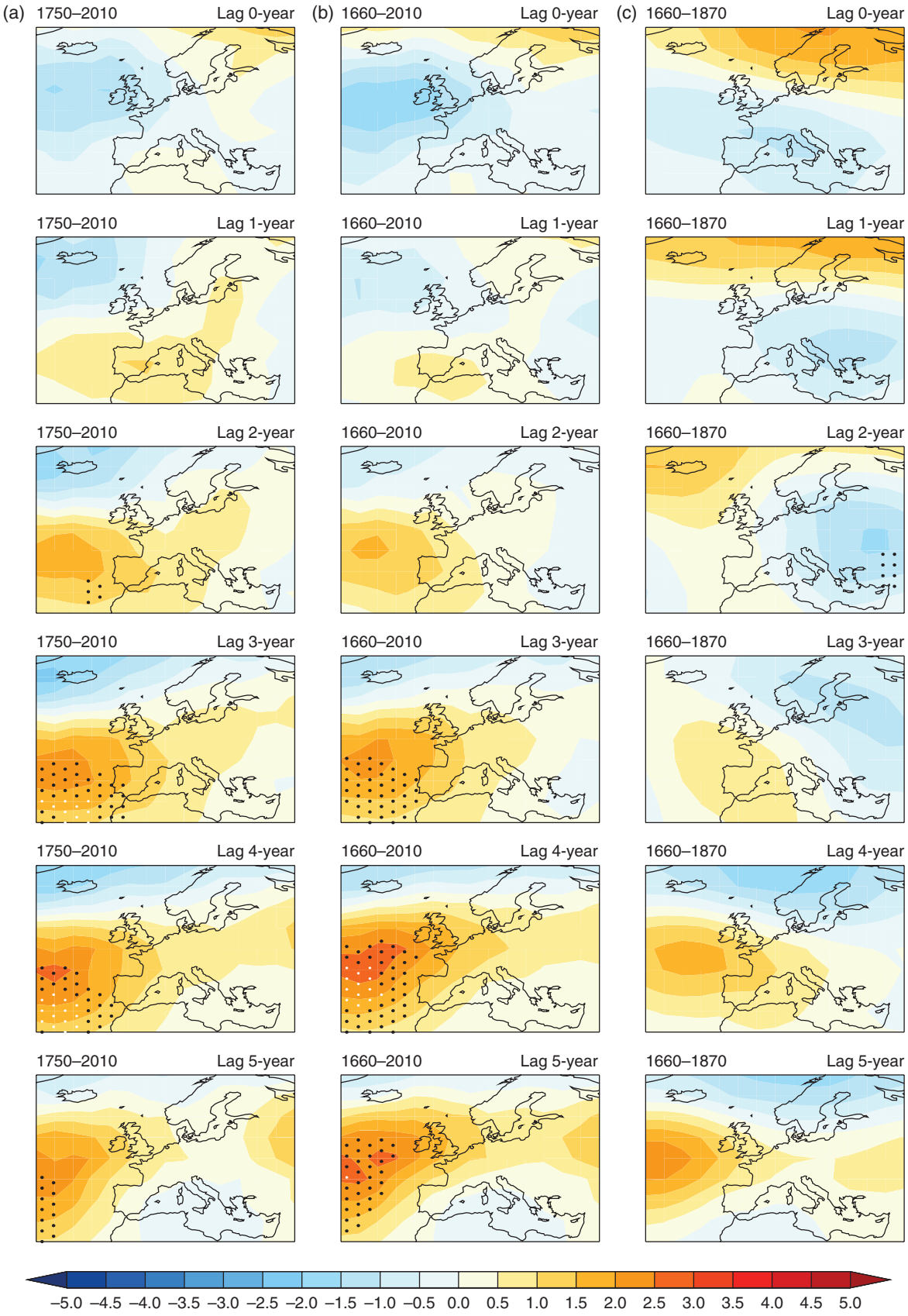

Figure 4. As Figure 3 but showing the solar cycle response from the regression analysis of the Luterbacher *et al.* (2002) reconstructed mean-sea-level pressure for the periods (a) 1750–2010, (b) 1660–2010 and (c) 1660–1870.

are more reliable (Luterbacher *et al.*, 1999, 2001, 2002). However, the reconstructed dataset extends back to 1660 and it is possible to obtain an estimate of solar variability in this earlier period if one employs the annual-averaged Group sunspot number. The results in Figure 4(b) are very similar to the shorter analyses, with a maximum response greater than 2.5 hPa at lag 4-years that peaks over the Azores with 99% statistical significance.

As a test of this extended analysis, Figure 4(c) shows results from only the first half of the data period (1660–1870; approx. 20 cycles) to examine its contribution (note that the contribution from the second half of the period is shown in Figure 4). Not surprisingly, given the reduced reliability of the data sources (both the SLP and the solar indices), the signal from the early part of the period is weaker and has little statistical significance. Nevertheless,

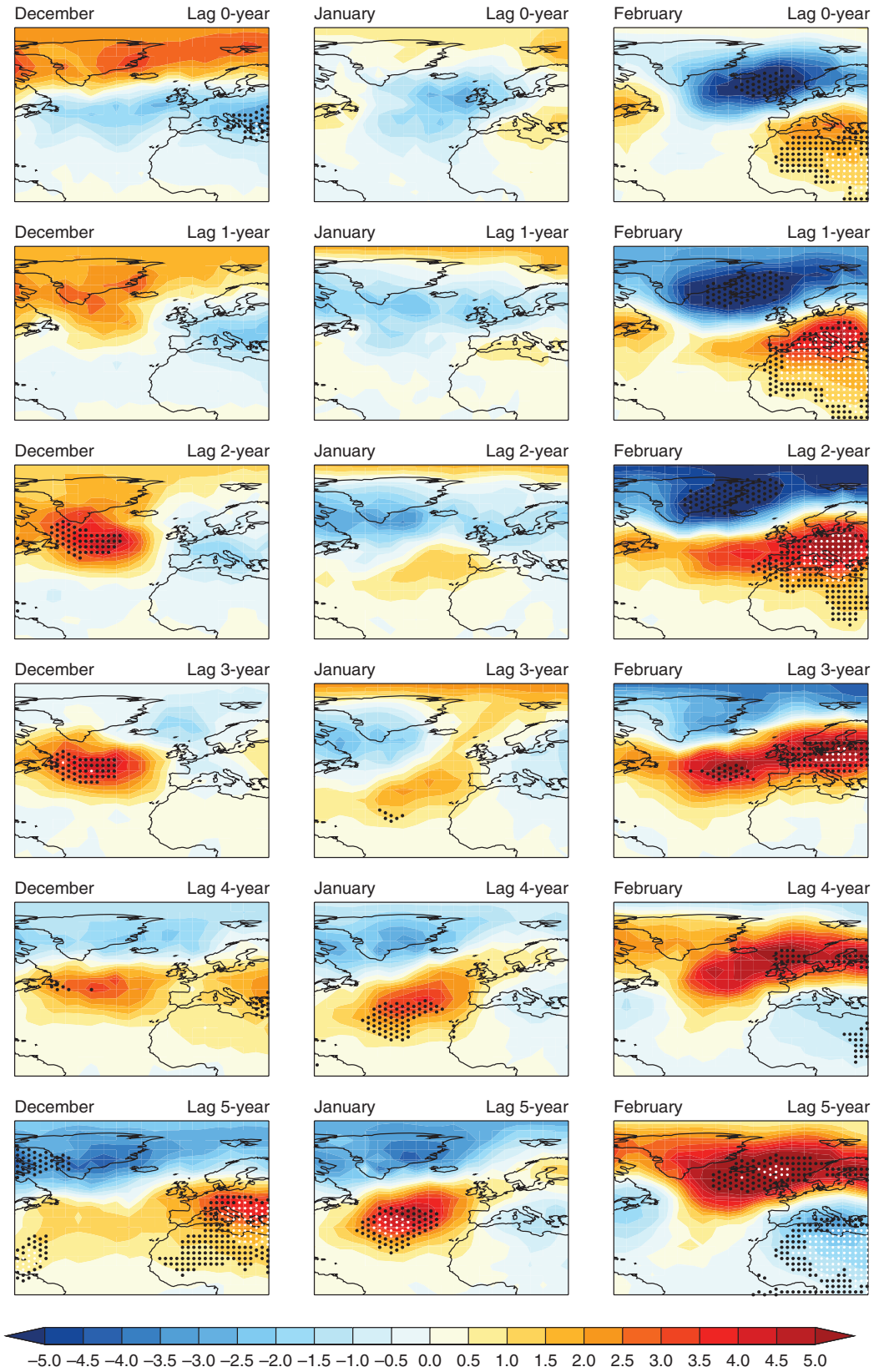

Figure 5. As Figure 3 but showing the 1870–2010 solar cycle response from the HadSLP regression analysis for the individual months December–February. The plotted region has been extended (in comparison to Figure 3) to show the full spatial extent of the Atlantic anomaly.

the patterns and their evolution over time are similar, with a clear signal developing over the Azores region between lags of 3 and 5 years.

3.2. *Monthly mean-sea-level pressure*

Analysis of seasonal mean responses provide a useful overview but can hide the impacts of competing processes, so it is important to examine the individual monthly contributions. This also helps to explain the subtle differences in responses at zero lag between G2013 who examined DJF averages and Brugnara *et al.* (2013) who examined JFM averages.

Figure 5 shows the 0–5 year lagged Smax–Smin solar responses for the individual December, January and February months. We now revert to focusing on the period 1870–2010 using the HadSLP datasets (corresponding to Figure 3 and the study of G2013) since (i) the HadSLP data have greater spatial coverage, so the full extent of the lagged Atlantic anomaly emerging in the region of

the Labrador Sea in December can be seen, (ii) the HadSLP data are more reliable, and (iii) ancillary data such as estimates of the ENSO and AMO are available for this period, allowing all relevant indices of variability (volcanic, ENSO, AMO, long-term trend and solar) to be included.

There are differences in Figure 5 between the evolving signals in each month that suggest more than one process is operating. The December response over the North Atlantic/European sector is most similar to the DJF average, with a statistically significant positive anomaly emerging over the southern tip of Greenland and the Labrador Sea region extending eastwards across the Atlantic at lags of 2–3 years. Continuing with discussion of the Azores region, a similar signal is present in January also, but is only significant at lags of 4–5 years. Thus the 3–4 year lagged response over the Azores region in the DJF average (Figure 3) arises primarily from the early-winter months (DJ) and the projection of the response onto the NAO in those months comes primarily from the signal in the southern part of the NAO, centred over the Azores.

In February there is a prominent statistically significant negative anomaly over the Icelandic region that emerges earlier, at lags 0–2 years with peak amplitude greater than −4 hPa, together with a significant positive anomaly over southern Europe and North Africa peaking at over 4 hPa with 99% statistical significance. This pattern also projects onto the NAO pattern but it maximises at 0–2 year lag (note that it has completely reversed in sign by lag 5 years) and it is only present in February. This is most likely the signal picked up by the Brugnara *et al.* (2013) analysis, since they analysed JFM averages and there are no statistically significant responses at lag zero in either January or March (not shown). Interestingly the pattern is displaced eastward from the standard NAO pattern, as also seen by W2010. A similar eastward displacement of the signal is also evident at lags of 4–5 years in December, so that signals at 4–5 year lags in December and February are of opposite sign and effectively cancel out in the DJF-averaged response.

Figure 6 shows the corresponding 11-year solar cycle response in SLP for the separate months December, January and February from the regression analysis of the much longer reconstruction data for 1660–2010. Although the dataset is clearly restricted geographically, the earlier data is of poorer quality and lack of available data prevents us from accounting for variability associated with ENSO and the AMO; it nevertheless shows the same characteristics as in Figure 5: the early-winter (December–January) response is lagged compared with the February response and the early and late winter responses at zero and 5-year lags are of opposite sign.

Examination of the individual months in Figures 5 and 6 thus indicates the possibility of two separate solar variability influence mechanisms, one primarily evident in early winter that has a 3–4 year lagged response and one primarily evident in late winter that emerges almost immediately. We suggest that these signals are consistent with currently proposed mechanisms for solar cycle influence at the surface.

The late winter (February) response can be explained by the so-called 'top-down' mechanism (Kodera, 1995; Haigh, 1996; Kodera and Kuroda, 2002; Matthes *et al.*, 2006; Gray *et al.*, 2010; Ineson *et al.*, 2011): stratospheric heating and circulation anomalies create an increased Equator-to-Pole temperature gradient and strengthened stratospheric polar vortex during Smax. This results in an anomalous positive Northern Annular Mode (NAM) structure in the lower stratosphere that extends to the surface (although the exact mechanism for this downward influence is still not fully understood: Baldwin and Dunkerton, 2001; Kidston *et al.*, 2015). This polar route of influence is likely to maximise its influence in late winter since major vortex disturbances (sudden stratospheric warmings) are more prevalent in late winter and there is also a time delay for the impact of the stratospheric anomaly to reach the surface. A solar influence mediated by the strength of the stratospheric polar vortex can thus explain the emergence of the late-winter signal at zero lag.

An additional top-down influence has been proposed via the impact of anomalous Equator-to-Pole temperature gradients on synoptic waves in the troposphere (Simpson *et al.*, 2009). An influence from this mechanism cannot be excluded; it acts all year round but could account for the peak response in February if the early-winter signal is obscured by ocean interactions, as discussed below.

The peak amplitude of the late-winter signal occurring at 1–2 year lags instead of at zero-lag can be partly attributed to uncertainty in which solar index is the optimum to employ in these studies. For example W2010 employed the open solar flux (Fs) index and Fs in general peaks around a year later than the sunspot number (Lockwood *et al.*, 2010). Sensitivity tests using Fs instead of sunspot number (not shown) generated a late-winter peak response a year earlier than with sunspot number. Nevertheless we choose to employ sunspot number in this analysis for consistency with previous studies and because of the long record of observations that are available. An additional mechanism that could produce a peak response at 1–2 year lag is the influence of energetic particle precipitation (Seppälä *et al.*, 2009).

The early-winter response, characterised by a lag of 3–4 years, has been the topic of recent papers (Scaife *et al.*, 2013; Andrews *et al.*, 2015; Thieblemont *et al.*, 2015). Although there is no obvious mechanism involving the atmosphere alone that can explain the substantial delay of 3–4 years seen in December and January, a positive NAO forcing from the atmosphere in each winter over several years around Smax will also influence the Atlantic SSTs, resulting in an associated SST anomaly. At the end of each winter this SST anomaly is subducted below the mixed layer (Alexander and Deser, 1995; Taws *et al.*, 2011) from where it can re-emerge the following winter. In this way, the NAO signal can be reinforced each year, with the result that the peak amplitude occurs at lags of approximately one-quarter cycle following Smax, i.e. after 3–4 years. The impact of this re-emerging SST signal is likely to be most evident in early winter and can therefore account for the 3–4 year lagged signal in December–January.

In Figure 7 the corresponding 0–5 year lagged Smax–Smin solar responses for the individual December, January and February months are shown for SSTs (the DJF averages are shown in figure 5 of G2013). The evolution in each month follows the pattern of the SLP anomalies in Figure 5, demonstrating how closely linked they are. In particular, the lag 0 response is seen in late winter while the early-winter response peaks at lags 2–3 years. There is a clear tripolar pattern of anomalies which is a typical response to sustained NAO forcing, with an anomalously cold tongue extending eastward from the Labrador Sea and warm anomalies to the north and south of this.

3.3. *Blocking frequency*

Having shown that the DJF solar response pattern in surface pressure appears to be a combination of two patterns, one dominating the early winter with a 3–4 year lag and one dominating the late winter with 0–2 year lag, we now analyse the blocking frequency dataset (see section 2) using the same multilinear regression technique, to explore whether similar lagged responses are also evident in the blocking frequency. This extends the analysis of W2010 by (i) using a regression approach instead of composites, thus reducing possible contamination from other forcing factors, (ii) examining the lagged response to the solar cycle, and (iii) examining the responses in the separate months as well as in the DJF average.

In addition to the standard indices included in the regression analysis (solar indices, volcanic aerosol, ENSO, AMO, trend) the analysis also includes two QBO terms (see section 2). Although the blocking dataset is available from 1948, we analyse the period 1953–2010 so we can include a QBO index using equatorial wind radiosonde observations that are available from 1953. This time

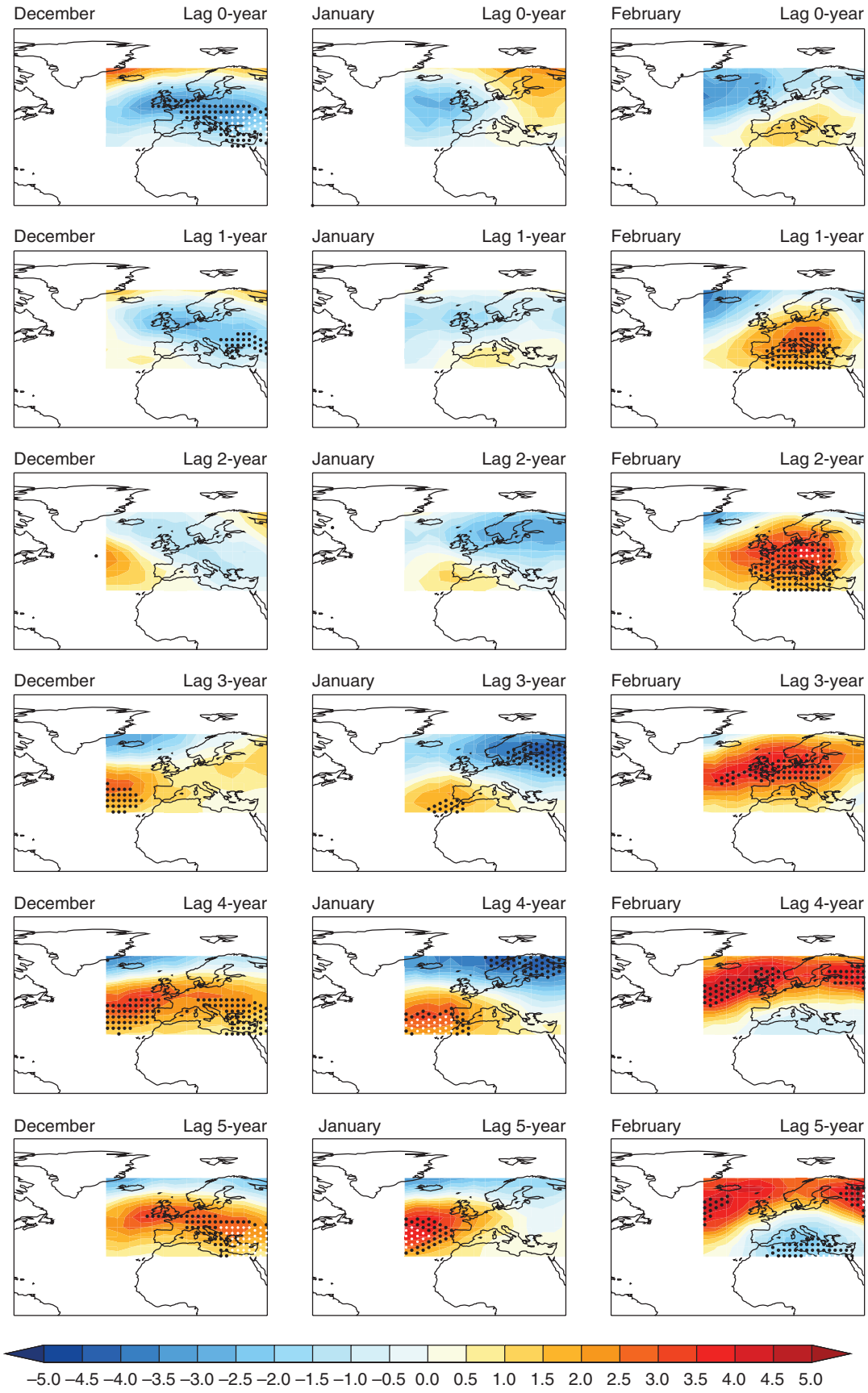

Figure 6. As Figure 5 but showing the 1660–2010 solar cycle response from the corresponding regression analysis of the Luterbacher *et al.* (2002) mean-sea-level pressure (hPa) dataset. Regions of white denote missing data; the horizontal extent of the plots is identical to Figure 5 for ease of comparison.

period also corresponds relatively closely to the period studied by W2010 (1958–2010).

As an initial check to ensure that the solar cycle signal is sufficiently well captured even in this shorter dataset, Figure 8(a) shows the DJF solar cycle SLP response over the European/Atlantic sector for 1953–2010. Comparison with Figures 4 and 5 confirms that this much shorter period also displays the same characteristics as the longer-period analyses. A positive NAO-like anomaly distribution is present at lag-zero but with no significance. At 1-year lags this signal has increased, with peak anomalies of ∼3 hPa centred over Iceland and ∼2.5 hPa over the Azores. The 1-year lagged response distribution and amplitude are similar to those

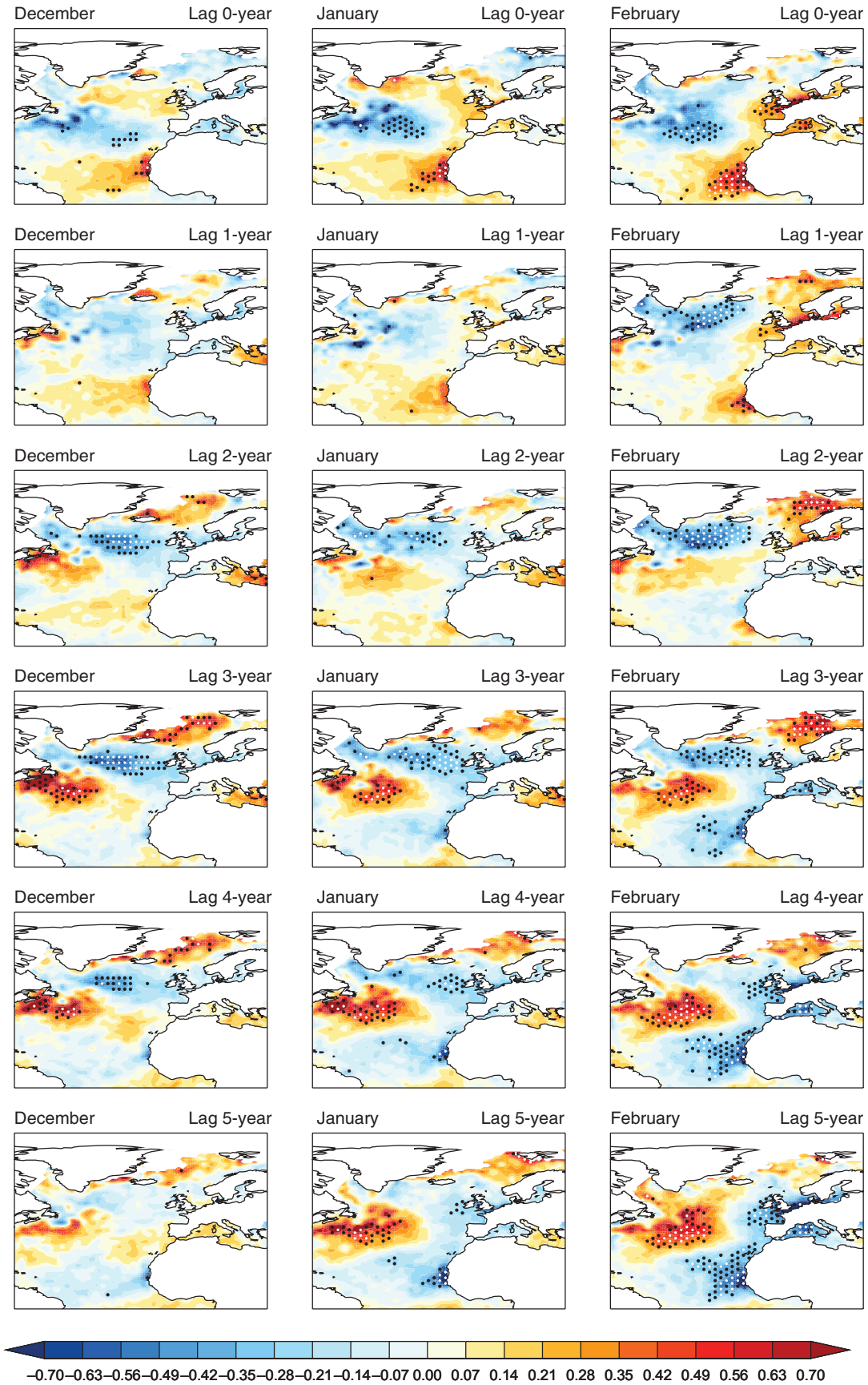

Figure 7. As Figure 5 but showing the 1870–2010 solar cycle response from the corresponding regression analysis of the HadISST sea-surface temperature (K) dataset.

found in the composite analysis of W2010 at lag-zero. This can be explained by the fact that W2010 employed the open solar flux Fs as their solar index, rather than the sunspot number used here. W2010 did not examine lagged signals, but Figure 8(a) shows that the response continues to grow in amplitude and increase its statistical significance over the Azores region, reaching a peak response at lags of 3 years. The positive anomaly also tilts southwest–northeast with increasing lag and extends across into northern Europe, similar to the response pattern in Figure 4.

The 11-year solar cycle signal in DJF blocking frequencies is shown in Figure 8(b). The main response is a negative anomaly centred over Iceland at lags 0–2 years. This indicates reduced blocking frequencies during Smax periods. The signal has 99% statistical significance and the sign of the anomaly has

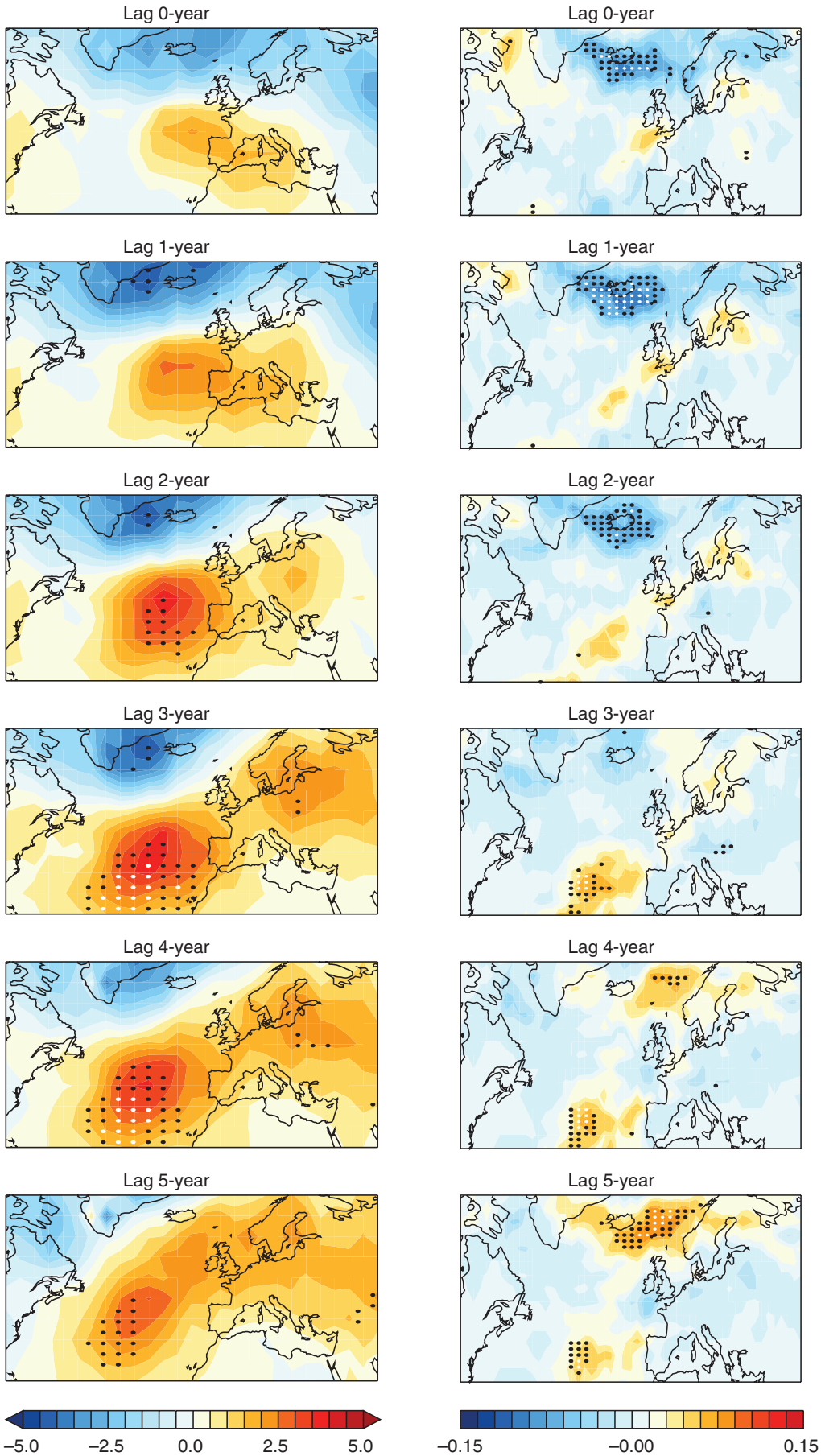

Figure 8. (a) As Figure 4 but showing the HadSLP DJF solar cycle response for the period 1953–2010. (b) DJF-averaged solar cycle response in blocking frequency (per day) for the period 1955–2010. The regression coefficients have been multiplied by the maximum difference in sunspot number between Smax and Smin over the time period to give an estimate of the maximum likely contribution over the time period. Black and white stippling shows regions of 95 and 99% statistical significance, respectively.

reversed by lag 5-years. The regression analysis includes all other available indices (i.e. volcanic, trend, ENSO, AMO, 2 × QBO) but sensitivity tests (not shown) confirm that the 11-year solar signal is not affected by their inclusion/exclusion. Using the whole available time series from 1948 (without the QBO) makes no substantial difference to the resulting signal. Note that the blocking index used here locates a block by the anticyclone, rather than the point of reversal as in the index used in W2010, hence the blocking anomaly is located slightly to the north when compared to W2010. In both cases the Smax anomaly corresponds to a reduction in the high-latitude blocking which, as shown by Scherrer *et al.* (2006) and Woollings *et al.* (2008), is characterised primarily by negative NAO events. At Smax the reduced blocking is centred over the Icelandic region; however, as noted by W2010, when compared with the climatological distribution in Figure 1(b), the Smin distribution (at 5-year lag) is centred more on the eastern side of the NAO-blocking region. A positive anomaly also develops over the Azores region and peaks at lag 3–5 years; however, blocking anomalies in this region should be treated with caution. Here the index identifies so-called Low-Latitude Blocking that can represent relatively subtle changes in the subtropical circulation (Davini *et al.*, 2012).

The primary blocking response at lags 0–2 years in Figure 8(b) resembles the time evolution of the late winter (JF) SLP response seen in Figure 5, so it is instructive to examine the solar cycle (SC) blocking signal in the individual months, to see whether the blocking response is also dominated by these late-winter months. Figure 9 shows the corresponding distributions for the individual months December through to February and confirms that the negative anomaly over Iceland does indeed originate primarily from the late winter (JF), similar to the SLP response. Indeed, in February the anomalous blocking region also extends across into Greenland. In December there is no significant change in blocking, suggesting that blocking frequency may not be directly connected to the lag 3–4 year lagged response in SLP.

An interesting feature of both the SLP and blocking responses in February is that the signal over the Icelandic/Greenland region at lags of 5 years, corresponding to the response at Smin, has higher statistical significance than at lag zero (and this is also true of lag 6-years compared with lag 1-year). This not only indicates that blocking frequencies are increased around the time of Smin but suggests that this response is more robust than the Smax response. This asymmetry in the response was also noted by W2010, but its cause is not clear. One possibility is that it is connected to the nonlinear behaviour of the stratospheric polar vortex, but this requires further investigation.

3.4. *Solar cycle blocking signal in context*

The results presented in section 3.3 suggest that a significant proportion of variability in blocking frequency can be attributed to the 11-year solar cycle. To place these results in perspective with the other major factors known to influence blocking in the Atlantic/European sector, Figure 10 shows the DJF regression coefficients associated with the ENSO and AMO indices employed in the multilinear regression analysis. Each distribution has been scaled to represent the maximum change in blocking frequency associated with each index. Thus the ENSO response can be interpreted as the maximum difference between El Niño/La Niña years (approximately 3.5 °C; see Figure 3) and the AMO response can be interpreted as the maximum likely difference between positive and negative AMO index years (i.e. warm minus cold Atlantic SST years; approximately 0.8 °C; see Figure 2). All signals are plotted at zero lag (i.e. an immediate response in the same year) apart from the solar cycle signal, which is plotted at 1-year lag since Figure 8 suggests that this is the time of greatest response amplitude.

The influences of the ENSO and AMO on blocking frequencies shown in Figure 10 compare well to previous studies. For example, a reduction in European blocking associated with positive ENSO was noted by Barriopedro *et al.* (2006). The AMO distribution agrees well with the analysis of Hakkinen *et al.* (2011), with increased blocking occurring from Greenland to the United Kingdom when North Atlantic SSTs are relatively warm and the sub-polar gyre is weak, with 95–99% statistical significance. We note that the 11-year solar signal is as large in amplitude as the ENSO and AMO signals and the region over which there is 99% significance is larger than either.

4. Summary and discussion

A multiple linear regression analysis has been performed to explore the 11-year solar cycle influence on mean-sea-level pressure and frequency of blocking over the Atlantic/European sector. The 3–4 year lagged solar response signal in the 1870–2010 record of DJF mean-sea-level pressure, first identified by Gray *et al.* (2013), has been confirmed in a much longer reconstructed time series spanning the period 1660–2010 (350 years; approximately 32 solar cycles; see Figure 4(b)). These results confirm that there is a tendency for positive NAO anomalies to follow solar maxima and negative NAO anomalies to follow solar minima. The signal peaks at a lag of ∼4 years with a maximum amplitude greater than 2.5 hPa and 99% statistical significance. Apparent inconsistencies of results from previous studies have been resolved and stem primarily from the lagged nature of the response and the differences between early-winter and late-winter responses.

Analysis of the individual months that contribute to the 1870–2010 DJF-averaged signal (Figure 5) shows two main features: (i) a 2–4 year lagged response in early winter whose peak amplitude is greater than +3 hPa over the Azores region with 95% statistical significance at 2–3 year lags in December, and (ii) a 0–2 year lagged response in late winter whose peak amplitude is greater than +4 hPa over southern Europe with 99% statistical significance and greater than −4.5 hPa over Iceland with 95% statistical significance at 2-year lag. The early-winter signal tends to dominate the DJF average, resulting in the observed 3–4 year lagged DJF response.

The results suggest that two different mechanisms may be operating and these are discussed in terms of the current proposed mechanisms for solar influence. The so-called 'top-down' influence from the atmosphere via heating effects in the stratosphere is suggested to explain the 0–2 year lagged response in late winter. This mechanism operates throughout the winter but maximises in late winter with an almost-immediate impact at the surface. The influence of this sustained top-down forcing of the NAO during each winter also has an influence on the sea-surface temperatures (SSTs). The SST anomaly present at the end of each winter is subducted below the mixed layer from where it can re-emerge in the following winter, thus reinforcing the NAO signal each year so that the peak amplitude occurs at lags of approximately one-quarter solar cycle, i.e. 3–4 years. The impact of this signal is likely to be most evident soon after it re-emerges, in early winter.

While both the early-winter and late-winter solar responses project onto the NAO, they each show distinct patterns that can potentially be used for model validation purposes and thus help to clarify the mechanisms. In particular, the early-winter signal 3–4 years after solar maximum is dominated by positive pressure anomalies over the southern region of the NAO, i.e. over the Atlantic and centred over the Azores. In contrast, the late-winter signal at 0–2 years after solar maximum shows both a negative response over the northern region of the NAO, centred over Iceland, as well as a positive response that is positioned further south and eastward, centred over southern Europe.

A corresponding analysis was performed to examine the 11-year solar signal in frequency of blocking events over the North Atlantic and Europe. The analysis confirmed previous results of Woollings *et al.* (2010) that showed increased DJF blocking frequency around periods of solar minimum, although these

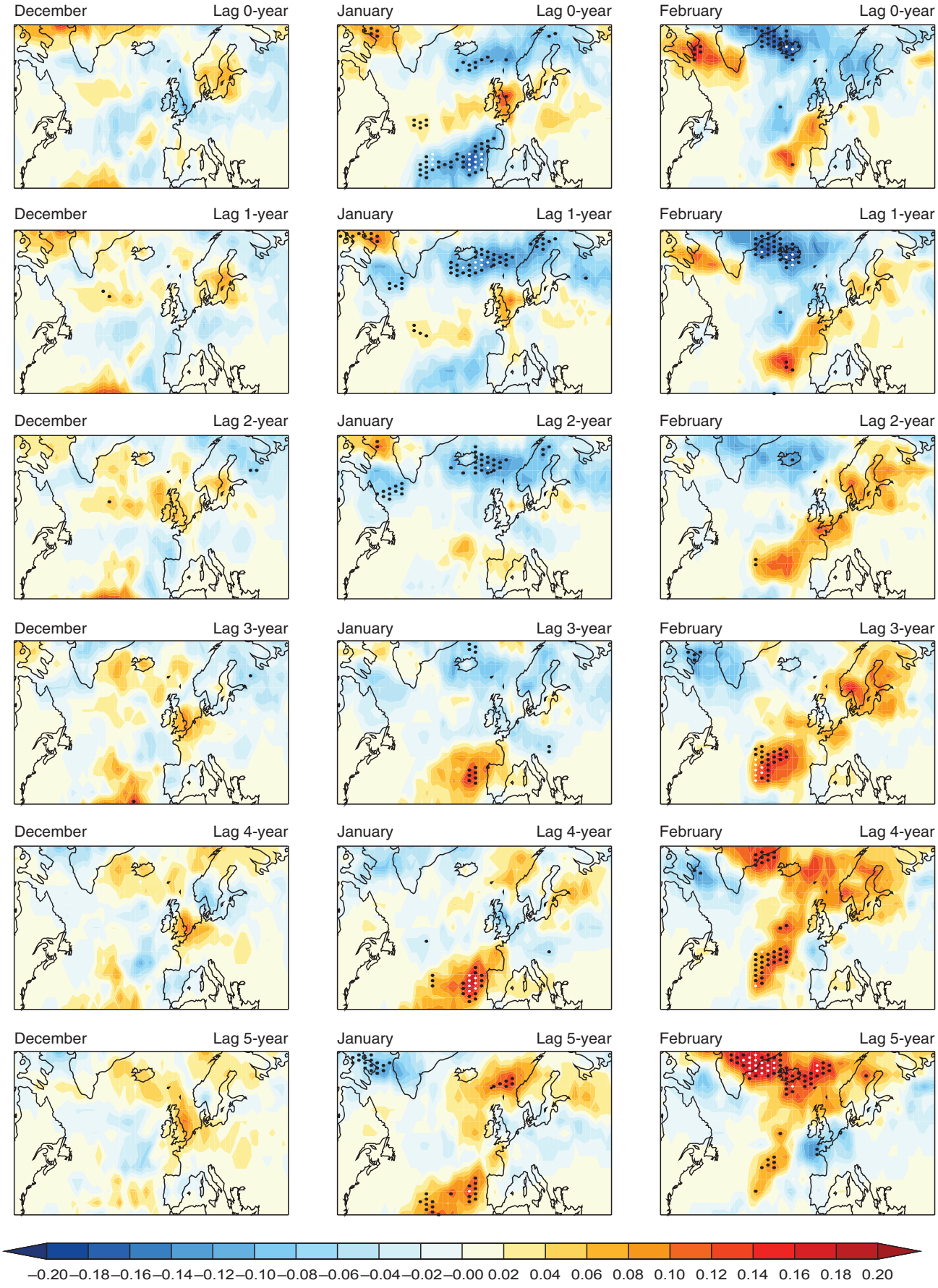

Figure 9. As Figure 8 but showing the 1953–2010 solar cycle response in blocking frequency for the individual months December–February.

results should be treated with caution since the analysed data span only 58 years. The maximum response (with 99% statistical significance; see Figure 8(b)) was found to occur over Iceland at 1-year lag, i.e. it does not display the 3–4 year lag seen in the SLP results. The DJF-averaged response was found to come primarily from the late-winter (JF) response, with no statistically significant influence seen in December. This suggests that the early-winter influence on the NAO via ocean feedbacks described above, which presumably influence the storm track, has little influence on the frequency of blocking. The late-winter influence lends support to earlier studies that suggest a stratosphere–blocking interaction (Woollings *et al.*, 2010) since the stratosphere also

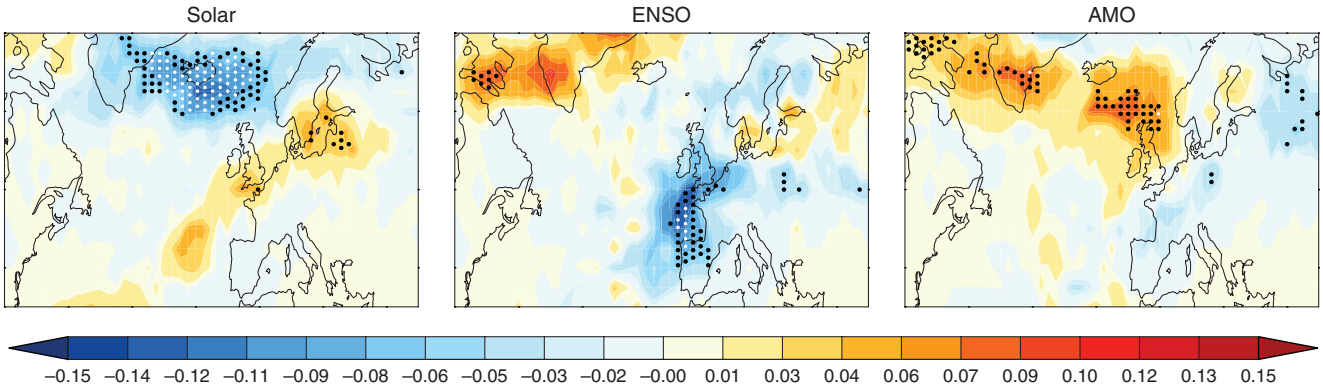

Figure 10. Results from the 1953–2010 regression analysis of DJF-averaged blocking frequency, showing the signal associated with variability in (a) sunspot number, (b) ENSO and (c) the AMO. The ENSO and AMO regression coefficients have been re-scaled to show the maximum likely response over this time period (i.e. the response to an ENSO/AMO change of approx. 3.5 and 0.8 °C respectively); the solar regression coefficients are scaled as in Figure 4, to show Smax minus Smin differences of 180 sunspot numbers.

responds to solar forcing almost immediately (Gray *et al.*, 2013; Mitchell *et al.*, 2015). However, we note that such short response lags (and the additional uncertainty in lag-times introduced by uncertainty in which solar index is best employed) mean that it is not possible to categorically distinguish cause from effect using only observational data. While the late-winter surface signal in SLP and blocking may be a response to top-down stratospheric forcing, it is also possible that the stratosphere could simply be responding to the change in blocking frequency caused by some other influence mechanism, since blocking events are associated with increased wave propagation into the stratosphere and have been identified as precursors to disturbances of the stratospheric vortex in winter. Well-designed model experiments are needed to clarify this.

The 11-year solar signal response was also compared with other known influences on blocking frequency over the Atlantic/European sector, namely from ENSO and the Atlantic Multidecadal Oscillation (AMO). The 11-year solar signal was found to be as large in amplitude as the ENSO and AMO signals and the region showing 99% statistical significance was larger than either (Figure 10). When blocking events occur over Iceland the effect on European temperatures can be particularly acute, so the potential to improve seasonal forecasting for European winters by taking account of the influence from the solar cycle is noted.

Acknowledgements

We thank the reviewers for their helpful comments. LJG was funded by the UK Natural Environmental Research Council (NERC) National Centre for Atmospheric Sciences (NCAS) and NERC grant NE/H024409/1 (Climate Change Predictions with a Fully Resolved Stratosphere).

References

Alexander MA, Deser C. 1995. A mechanism for the recurrence of wintertime midlatitude SST anomalies. *J. Phys. Oceanogr.* **25**: 122–137, doi: 10.1175/1520-0485(1995)025<0122:AMFTRO>2.0.CO;2.

Allan RJ, Ansell TJ. 2006. A new globally complete monthly historical gridded mean sea level pressure data set (HadSLP2): 1850–2004. *J. Clim* **19**: 5816–5842, doi: 10.1175/JCLI3937.1.

Andrews MB, Knight JR, Gray LJ. 2015. A simulated lagged response of the North Atlantic Oscillation to the solar cycle over the period 1960–2009. *Environ. Res. Lett.* **10**: 054022, doi: 10.1088/1748-9326/10/5/054022.

Baldwin MP, Dunkerton TJ. 2001. Stratospheric harbingers of anomalous weather regimes. *Science* **294**: 581, doi: 10.1126/science.1063315.

Barriopedro D, García-Herrera R, Lupo AR, Hernández E. 2006. A climatology of Northern Hemisphere blocking. *J. Clim* **19**: 1042–1063.

Barriopedro D, Garcia-Herrera R, Huth R. 2008. Solar modulation of Northern Hemisphere winter blocking. *J. Geophys. Res.* **113**: D14118, doi: 10.1029/2008JD009789.

Brugnara Y, Bronnimann S, Luterbacher J, Rozanov E. 2013. Influence of sunspot cycle on the Northern Hemisphere wintertime circulation from long upper-air data sets. *Atmos. Chem. Phys.* **13**: 6275–6288, doi: 10.5194/acp-13-6275-2013.

Crooks SA, Gray LJ. 2005. Characterisation of the 11-year solar signal using a multiple regression analysis of the ERA-40 data set. *J. Clim.* **18**: 996–1015, doi: 10.1175/JCLI-3308.1.

Davini P, Cagnazzo C, Gualdi S, Navarra A. 2012. Bidimensional diagnostics, variability, and trends of Northern Hemisphere blocking. *J. Clim* **25**: 6496–6509.

Enfield DB, Mestas-Nuñez AM, Trimble PJ. 2001. The Atlantic Multidecadal Oscillation and its relation to rainfall and river flows in the continental U.S. *Geophys. Res. Lett.* **28**: 2077–2080, doi: 10.1029/2000GL012745.

Gray LJ, Beer J, Geller M, Haigh JD, Lockwood M, Matthes K, Cubasch U, Fleitmann D, Harrison G, Hood L, Luterbacher J, Meehl GA, Shindell D, van Geel B, White W. 2010. Solar influences on climate. *Rev. Geophys.* **48**: RG4001, doi: 10.1029/2009RG000282.

Gray LJ, Scaife AA, Mitchell DM, Osprey S, Ineson S, Hardiman S, Butchart N, Knight J, Sutton R, Kodera K. 2013. A lagged response to the 11 year solar cycle in observed winter Atlantic/European weather patterns. *J. Geophys. Res.* **118**: 13405–13420, doi: 10.1002/2013JD020062.

Haigh JD. 1996. The impact of solar variability on climate. *Science* **272**: 981–984, doi: 10.1026/science.272.5264.981.

Hakkinen S, Rhines PB, Worthen DL. 2011. Atmospheric blocking and Atlantic multidecadal ocean variability. *Science* **334**: 655–659, doi: 10.1126/science.1205683.

Ineson S, Scaife AA, Knight JR, Manners JC, Dunstone NJ, Gray LJ, Haigh JD. 2011. Solar forcing of winter climate variability in the Northern Hemisphere. *Nat. Geosci.* **4**: 753–757, doi: 10.1038/ngeo1282.

Kalnay E, Kanamitsu M, Kistler R, Collins W, Deaven D, Gandin L, Iredell M, Saha S, White G, Woollen J, Zhu Y, Leetmaa A, Reynolds R, Chelliah M, Ebisuzaki W, Higgins W, Janowiak J, Mo KC, Ropelewski C, Wang J, Jenne R, Joseph D. 1996. The NCEP/NCAR 40-year reanalysis project. *Bull. Am. Meteorol. Soc.* **77**: 437–471.

Kidston J, Scaife AA, Hardiman SC, Mitchell DM, Butchart N, Baldwin MP, Gray LJ. 2015. Stratospheric influence on tropospheric jet streams, storm tracks and surface weather. *Nat. Geosci.* **8**: 433–440, doi: 10.1038/ngeo2424.

Knudsen MF, Jacobsen BH, Seidenkrantz M-S, Olsen J. 2014. Evidence for external forcing of the Atlantic Multidecadal Oscillation since termination of the Little Ice Age. *Nat. Commun.* **5**: 3323, doi: 10.1038/ncomms4323.

Kodera K. 1995. On the origin and nature of interannual variability of the winter stratosphere circulation in the Northern Hemisphere. *J. Geophys. Res.* **100**: 14077–14087, doi: 10.1029/95JD01172.

Kodera K, Kuroda Y. 2002. Dynamical response to the solar cycle: Winter stratopause and lower stratosphere. *J. Geophys. Res.* **107**: 4749, doi: 10.1029/2002JD002224.

Kuttel M, Xoplaki E, Gallego D, Luterbacher J, Garcia-Herrera R, Allan R, Barriendos M, Jones PD, Wheeler D, Wanner H. 2010. The importance of ship log data: Reconstructing North Atlantic, European and Mediterranean sea level pressure fields back to 1750. *Clim. Dyn.* **34**: 1115–1128, doi: 10.1007/s00382-0009-0577-9.

Lockwood M, Harrison RG, Woollings T, Solanki S. 2010. Are cold winters in Europe associated with low solar activity? *Environ. Res. Lett.* **5**: 024001, doi: 10.1088/1748-9326/5/2/024001.

Luterbacher J, Schmutz C, Gyalistras D, Xoplaki E, Wanner H. 1999. Reconstruction of monthly NAO and EU indices back to AD 1675. *Geophys. Res. Lett.* **26**: 2745–2748, doi: 10.1029/1999GL900576.

Luterbacher J, Xoplaki E, Dietrich D, Jones PD, Davies T, Portis D, Gonzalez JF, von Storch H, Gyalistras D, Casty C, Wanner H. 2001. Extending North Atlantic Oscillation constructions back to 1500. *Atmos. Sci. Lett.* **2**: 114–124, doi: 10.1006/asle.2002.0047.

Luterbacher J, Xoplaki E, Dietrich D, Rickli R, Jacobeit J, Beck C, Gyalistras D, Schmutz C, Wanner H. 2002. Reconstruction of sea level pressure fields over the eastern North Atlantic and Europe back to 1500. *Clim. Dyn.* **18**: 545–561.

Matthes K, Kuroda Y, Kodera K, Langematz U. 2006. Transfer of the solar signal from the stratosphere to the troposphere: Northern winter. *J. Geophys. Res.* **111**: D06108, doi: 10.1029/2005JD006283.

Menary MB, Scaife AA. 2014. Naturally forced multidecadal variability of the Atlantic meridional overturning circulation. *Clim. Dyn.* **42**: 1347–1362, doi: 10.1007/s00382-013-2028.

Mitchell DM, Gray LJ, Fujiwara M, Hibino T, Anstey JA, Ebisuzaki W, Harada Y, Long C, Misios S, Stott PA, Tan D. 2015. Signatures of naturally induced variability in the atmosphere using multiple reanalysis datasets. *Q. J. R. Meteorol. Soc.* **141**: 2011–2031, doi: 10.1002/qj.2492.

Rayner NA, Parker DE, Horton EB, Folland CK, Alexander LV, Rowell DP, Kent EC, Kaplan A. 2003. Global analyses of sea surface temperature, sea ice and night marine air temperature since the late nineteenth century. *J. Geophys. Res.* **108**: 4407, doi: 10.1029/2002JD002670.

Roy I, Haigh JD. 2010. Solar cycle signals in sea level pressure and sea surface temperature. *Atmos. Chem. Phys.* **10**: 3147–3153.

Scaife AA, Ineson S, Knight JR, Gray LJ, Kodera K, Smith DM. 2013. A mechanism for lagged North Atlantic climate response to solar variability. *Geophys. Res. Lett.* **40**: 434–439, doi: 10.1002/grl.50099.

Sato M, Hansen J, McCormick M, Pollack J. 1993. Stratospheric aerosol optical depths. *J. Geophys. Res.* **98**: 22987–22994, doi: 10.1029/93JD02553.

Scherrer SC, Croci-Maspoli M, Schwierz C, Appenzeller C. 2006. Two-dimensional indices of atmospheric blocking and their statistical relationship with winter climate patterns in the Euro-Atlantic region. *Int. J. Climatol.* **26**: 233–249.

Seppälä A, Randall CE, Clilverd MA, Rozanov EV, Rodger CJ. 2009. Geomagnetic activity and polar surface air temperature variability. *J. Geophys. Res.* **114**: A10312, doi: 10.1029/2008JA014029.

Simpson I, Blackburn M, Haigh JD. 2009. The role of eddies in driving the tropospheric response to stratospheric heating perturbations. *J. Atmos. Sci.* **66**: 1347–1365.

Taws SL, Marsh R, Wells NC, Hirschi J. 2011. Re-emerging ocean temperature anomalies in late-2010 associated with a repeat negative NAO. *Geophys. Res. Lett.* **38**: L20601, doi: 10.1029/2011GL048978.

Thieblemont R, Matthes K, Omrani N-E, Kodera K, Hansen F. 2015. Solar forcing synchronizes decadal North Atlantic climate variability. *Nat. Commun.* **6**: 8268, doi: 10.1038/ncomms9268.

Woollings T, Hoskins BJ, Blackburn M, Berrisford P. 2008. A new Rossby wave-breaking interpretation of the North Atlantic Oscillation. *J. Atmos. Sci.* **65**: 609–626.

Woollings T, Lockwood M, Masato G, Bell C, Gray LJ. 2010. Enhanced signature of solar variability in Eurasian winter climate. *Geophys. Res. Lett.* **37**: L20805, doi: 10.1029/2010GL044601.

Woollings T, Franzke C, Hodson DLR, Dong B, Barnes EA, Raible CC, Pinto JG. 2014. Contrasting interannual and multidecadal NAO variability. *Clim. Dyn.* **45**: 539–556.